A Journal of the Gesellschaft Deutscher Chemiker

Angewandte International Edition GDCh Chemie

www.angewandte.org

Accepted Article

Title: Increasing the Number of Aluminum Atoms in T3 Sites of a Mordenite Zeolite by a Low-pressure SiCl4 Treatment to Catalyze Dimethyl Ether Carbonylation

Authors: Rongsheng Liu, Benhan Fan, Wenna Zhang, Linying Wang, Liang Qi, Yingli Wang, Shutao Xu, Zhengxi Yu, Yingxu Wei, and Zhongmin Liu

To be cited as: *Angew. Chem. Int. Ed.* **2022**, e202116990

Link to VoR: https://doi.org/10.1002/anie.202116990

WILEY-VCH

10.1002/anie.202116990

WILEY-VCH

RESEARCH ARTICLE

Increasing the Number of Aluminum Atoms in T_3 Sites of a Mordenite Zeolite by a Low-pressure $SiCl_4$ Treatment to Catalyze Dimethyl Ether Carbonylation

Rongsheng Liu,[a, b] Benhan Fan,[a, b] Wenna Zhang,[a] Linying Wang,[a] Liang Qi,[a] Yingli Wang,[a] Shutao Xu,[a] Zhengxi Yu,*[a] Yingxu Wei,[a] and Zhongmin Liu*[a, b]

Rongsheng Liu and Benhan Fan contributed equally to this work.

[a] R. Liu, B. Fan, W. Zhang, L. Wang, L. Qi, Y. Wang, S. Xu, Z. Yu, Y Wei, Z. Liu
National Engineering Laboratory for Methanol to Olefins, Dalian National Laboratory for Clean Energy
Dalian Institute of Chemical Physics, Chinese Academy of Sciences
Dalian 116023, China
E-mail: zhengxiyu@dicp.ac.cn; liuzm@dicp.ac.cn
[b] R. Liu, B. Fan, Z. Liu
University of Chinese Academy of Sciences
Beijing 100049, China

Supporting information for this article is given via a link at the end of the document.

Abstract: Controlling the location of aluminum atoms in zeolite framework is critical for understanding structure-performance relationships of catalytic reaction systems and tailoring catalyst design. Herein, we report a strategy to preferentially relocate mordenite (MOR) framework Al atoms into the desired T_3 sites by low-pressure $SiCl_4$ treatment (LPST). High-field ^{27}Al NMR was used to identify the exact location of framework Al for the MOR samples. The results indicate that 73% of the framework Al atoms were at the T_3 sites after LPST under optimal conditions, which leads to controllably generating and intensifying active sites in MOR zeolite for dimethyl ether (DME) carbonylation reaction with higher methyl acetate (MA) selectivity and much longer lifetime (25 times). Further research reveals that the Al relocation mechanism involves simultaneous extraction, migration, and reinsertion of Al atoms from and into the parent MOR framework. This unique method is potentially applicable to other zeolites to control Al location.

Introduction

Zeolites have been widely applied in adsorption separation, ion exchange, and heterogeneous catalysis.[1] The frameworks of aluminosilicate zeolites are formed by corner-sharing SiO_4 and AlO_4 tetrahedra,[2] in which AlO_4 tetrahedra introduce excess negative charges and require extra-framework cations such as protons for charge compensation, leading to the formation of Brønsted acid sites (BASs).[3] The location of acidity-related Al atoms in the zeolite framework has a significant influence on the physicochemical performances of the zeolite. Therefore, understanding and further controlling the location of framework Al are of critical importance, being a common interesting matter for establishing zeolite structure-performance relationships and for rational catalyst design.[4]

Mordenite (MOR), one of the most important zeolites widely used as catalysts, consists of parallel 12- and 8- membered ring (MR) channels (7.0 × 6.5 and 5.7 × 2.6 Å) connected by 8-MR openings (4.8 × 3.4 Å) (so-called side pockets).[5] There are four crystallographically nonequivalent tetrahedra sites (T_1-T_4) in the MOR framework, in which the T_1, T_2, and T_4 sites are in the 12-MR main channel and the T_3 sites are inside the 8-MR channel (Figure S1).[5b, 6] The BASs in different positions show distinct confinement effects for catalytic reactions. It was reported that the 8-MR channel of MOR zeolite, rather than a large 12-MR channel, is a preferential location for many small molecule transformations, especially for the dimethyl ether (DME) carbonylation to methyl acetate (MA) reaction.[7] Corma et al. indicated that the T_3-O_{33} site in 8-MR channels is the only position for DME carbonylation by theoretical methods.[8] However, the BASs in the 12-MR channel cause coke formation reaction and deactivation of MOR zeolite.[7a, 7d, 9] As the DME carbonylation to MA reaction is a meaningful new way for transforming C_1 feedstock to C_2 oxygenates, and the reaction itself is very interesting for its high sensitivity to BASs positions in MOR zeolite,[5a, 10] it is essential to selectively generate and intensify active sites in 8-MR channels via placing framework Al into T_3 sites, not only for a better catalytic performance but also for a deep understanding of the reaction.

Many researchers have established new synthetic methods that combine different Al and Si sources, organic structure-directing agents (OSDAs), and inorganic compensating cations to control Al siting in different zeolite frameworks, such as MFI,[11] CHA,[12] FER,[13] and RTH,[14] but less for MOR zeolite.[5a, 15] And the variation of the Al siting is often limited by the synthetic parameters. The rational design of synthetic parameters to selectively place Al into the desired sits remains elusive. Post-synthesis methods were also explored to pursue the desired Al siting for specific applications.[16] For instance, it has been reported that Al atoms were introduced into T-sites of zeolites via $AlCl_3$ treatment (so-called alumination) by the reaction between $AlCl_3$ and silanol defects of the zeolite.[17] Post-treatments, such as steaming, chemical etching, employed to tune framework compositions by removing Al atoms, have been investigated extensively.[18] These treatments, usually based on random extraction or insertion of Al atoms from or into the zeolite framework, are difficult to control Al siting. $SiCl_4$ treatment has been used as an effective route for isomorphous substitution of Si for Al over zeolite framework with the release of $AlCl_3$ in some cases.[19] However, the method is difficult to apply directly to MOR zeolite owing to the diffusion limitations imposed by its one-dimensional 12-MR channels.[20] Up to now, there is still lacking

10.1002/anie.202116990

an effective strategy for controlling the location of framework Al in MOR zeolite.

The objective of this study is to explore whether the Al atoms in MOR zeolite can be selectively directed into the positions (T_3 sites) favorable to the DME carbonylation from other undesired ones via post $SiCl_4$ treatment under low-pressure conditions and with small MOR crystals to avoid diffusion limitations. We expected that, after Al replaced by Si in the 12-MR channel, the in-situ generated $AlCl_3$ could further take alumination effect to insert more Al atoms into T_3 sites in the 8-MR channel of MOR zeolite.

Herein, we have demonstrated that the framework Al can be directionally relocated among the different T-sites of the MOR zeolite through a low-pressure $SiCl_4$ treatment (LPST). The mechanism of directing Al into T_3 sites was proposed as Scheme 1. Due to the restriction of the molecular size, $SiCl_4$ selectively accesses the 12-MR channel and replaces framework Al by Si with the extraction of $AlCl_3$, and the $AlCl_3$ could migrate into the 8-MR channels and further react with silanol defects in the T_3 sites to reinsert Al into the zeolite framework. The results help to develop the strategies to obtain the zeolite with the optimal framework Al siting and highly desired active sites.

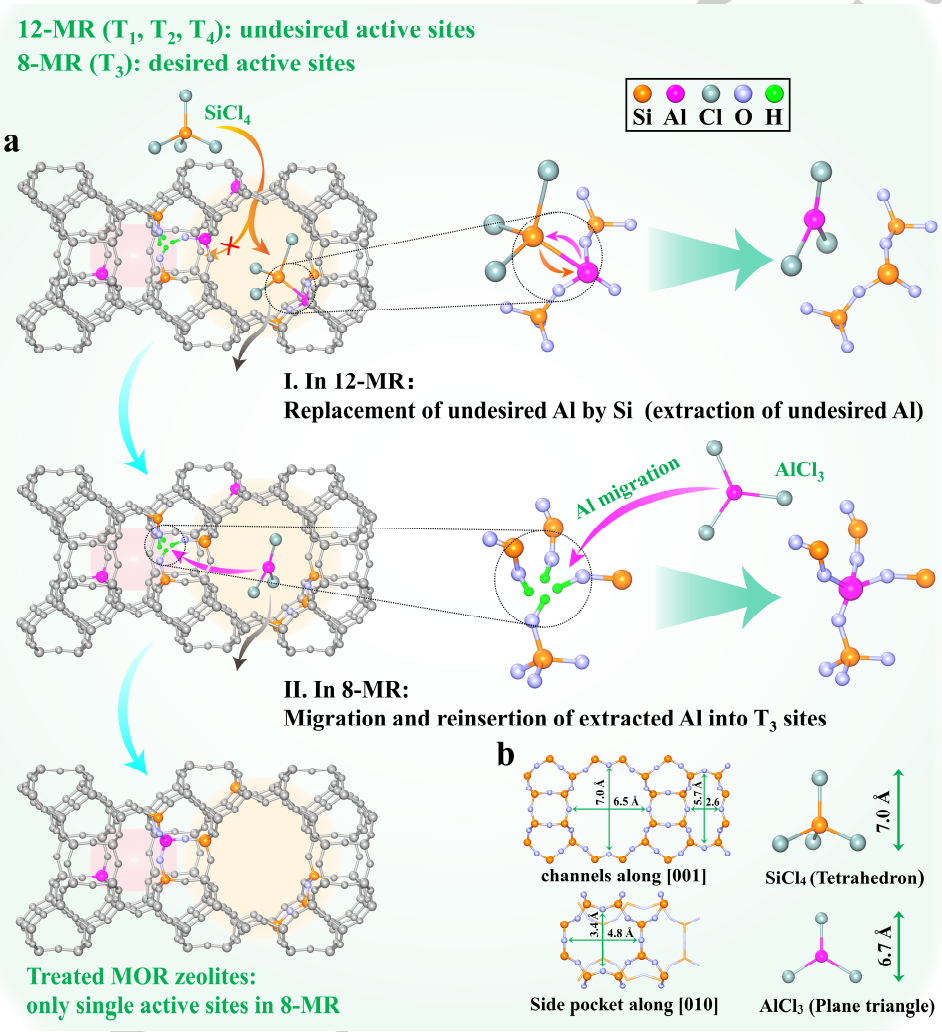

Scheme 1. a) Sketch map of a typical treatment process, showing the directional migration of framework Al into T_3 sites of the MOR zeolite via LPST. b) The topology of MOR and the steric configuration of $SiCl_4$ and $AlCl_3$ molecules with a kinetic diameter of 7.0 and 6.7 Å, respectively.

Results and Discussion

A lab-synthesized small size MOR zeolite (Figure S2) was used as the parent sample to exemplify the feasibility of the LPST strategy proposed in this work. Four treated samples were achieved under different LPST conditions (main difference in treatment temperature) to determine the impact on the location of framework Al and catalytic performance. The surface morphologies and particle sizes of the as-made MOR samples were tested with SEM (Figure S3). All the samples show similar morphologies, well-separated and uniform block-shaped particles (length: ~200nm, width: ~50 nm), and the uniformity of all samples could further be reflected in the similar N_2 adsorption-desorption isotherms (Figure S4), indicating that the LPST has no effect on the morphology and pore structure of the samples.

As compared with the treated samples (Figure S5), the parent MOR shows similar XRD peak intensities at higher diffraction angles, evidencing the intact maintenance of the zeolite structure. The peak intensity at the lower angle (2θ = 10°) range increased obviously after treatment. As shown in the IR result presented below (Figure 1), this lower intensity of the parent sample should be due to the existence of silanol defects, which might be healed during reaction with $SiCl_4$.[21]

10.1002/anie.202116990

RESEARCH ARTICLE

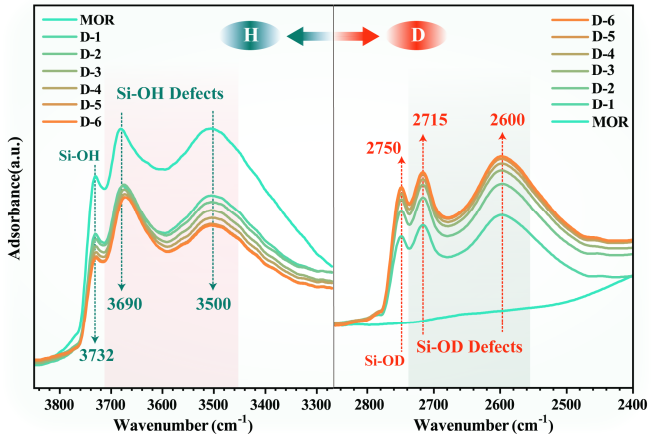

Figure 1. In-situ DRIFT spectra of H/D isotope exchange reaction using pyridine-d5 on the parent MOR zeolite at 423K: (left) O-H stretching region (3800-3300 cm^{-1}) and (right) O-D stretching region (2900-2400 cm^{-1}). H/D isotope exchanged circulations include: pyridine-d5 adsorption, H/D exchange reaction, and pyridine-d5 desorption. The digits in the sample codes represent the number of isotope exchange circulations.

Diffuse reflectance infrared Fourier transport (DRIFT) spectrum of parent MOR sample shows apparent signals in the O-H stretching vibration region (3800-3300 cm^{-1}) (Figure 1). The band at 3732 cm^{-1} is assigned to the terminal silanol groups, and the broad bands at around 3500 and 3690 cm^{-1} are associated with silanol groups inside defects.[10b, 17e] The distribution of silanol defects was further detected with in-situ DRIFT spectra after hydrogen-deuterium (H/D) isotope exchange (Figure 1). The pyridine-d5 molecule was chosen as probe molecular to selective H/D isotope exchange since its kinetic diameter (0.58 nm) only allows it to access the 12-MR channels of MOR.[7a] After the H/D isotope exchange, the corresponding silanol defects (Si-OD) bands, corresponding to 12-MR, were seen at 2600 and 2715 cm^{-1} in the O-D stretching region (2900-2400 cm^{-1}).[22] The rest of the signals at 3500 and 3690 cm^{-1} can be regarded as silanol defects in 8-MR channels. It is noteworthy that the H/D isotope exchange reaction was repeated 6 times until the signals corresponding to silanol defects showing no more changes to ensure that almost all the silanol groups (Si-OH) inside defects in the 12-MR are completely D-exchanged to silanol groups (Si-OD). Based on deconvolution of the DRIFT spectrum of D-6 (Figure S6), about half of silanol defects (52%) are in 8-MR channels, mainly related to T_3 sites. And the rest of the silanol defects are inside 12-MR channels of the parent MOR materials.

The change of silanol defects of parent MOR sample after LPST was studied by FTIR spectra (Figure S7a). The spectrum of the parent sample shows broad peaks from 3700 to 3200 cm^{-1}, which are related to silanol defects.[17e] After treatment, these broad signals disappeared in the spectra of the treated MOR samples, indicating that silanol defects, within both 8-MR and 12-MR channels, are healed during LPST. In the treated process, both directly fed $SiCl_4$ and in-situ generated $AlCl_3$ can consume the silanol defects, reported by various researchers.[17a, 21] Another related phenomenon is that a significant increase in the Si/Al ratio of the treated samples was observed through XRF analysis (Table S1), which could be caused by the growth of Si or removal of Al atoms into or from the zeolite framework during LPST. Moreover, the existence of two distinct channels containing four nonequivalent T-sites for MOR zeolite makes the whole chemistry even more complicated, and therefore, a detailed investigation on the evolution of zeolite framework compositions is needed to understand such a process.

Figure 2 shows ^{29}Si and ^{1}H-^{29}Si cross-polarization (CP) MAS NMR spectra of the parent and treated MOR samples. In the ^{29}Si NMR (Figure 2a), the main peaks from -110 to -116 ppm can be assigned to Q^4, $Si(OSi)_4$, which were observed as shoulder peaks owing to the incoordination environment of four T-sites of MOR zeolite. The signals at around -106 and -102 ppm are attributed to $Si(OAl)(OSi)_3$ and Q^3 $Si(OH)(OSi)_3$ species, respectively. And the signal at -99 ppm, related to the $Si(OAl)_2(OSi)_2$, is negligible.[21, 23] With increasing treatment temperature, the ^{29}Si NMR spectra show that the $Si(OAl)(OSi)_3$ resonance signals exhibited an overall decreasing trend while the intensity of the Q^4 signal peaks increased correspondingly, suggesting that Al atoms are removed from the framework and Si are incorporated into the framework, namely the occurrence of isomorphous substitution of Si for Al in MOR during the LPST.

Moreover, an apparent splitting of the Q^4 resonance peaks of ^{29}Si NMR spectra was observed after LPST. For detailed information of the framework Si location, the Q^4 was deconvoluted to three signals at around -112.8, -113.5, and -115.3 ppm, attributed to framework Si in T_1, T_3, and T_2+T_4 sites, respectively (Figure 2b), in terms of the result reported by Klinowski.[24] The relevant quantitative results of ^{29}Si NMR spectra are listed in Table S3. It was observed that the increment of Q^4 signals is mainly related to T_2+T_4 sites, especially at lower temperatures (Figure 2c), indicating that the incorporation of Si in T_2+T_4 sites preferentially occurs in the 12-MR channels during LPST.

10.1002/anie.202116990

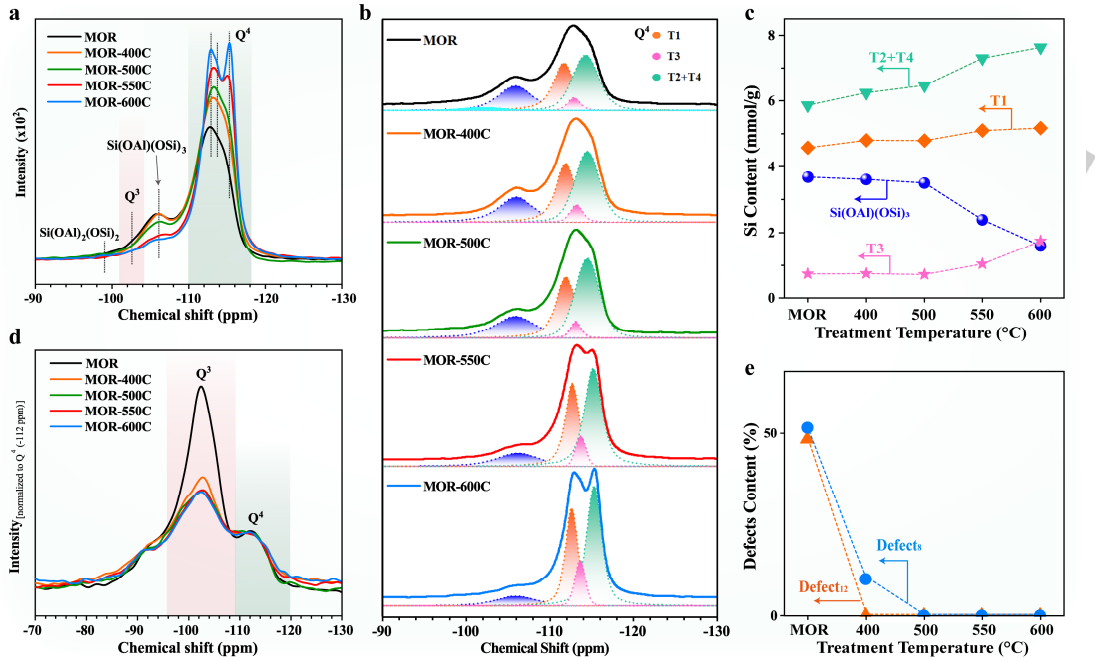

Figure 2. ^{29}Si MAS NMR (a) and ^{1}H-^{29}Si cross-polarization (CP) MAS NMR (d) spectra of as-made samples. b) Deconvolution of the ^{29}Si MAS NMR spectra of all samples. The evolution of zeolite framework Si atoms (c) and silanol defects (e) with increasing treatment temperature and the provided data of framework Si content was based on the combination of XRF and ^{29}Si MAS NMR. The data of silanol defects content was acquired from ^{29}Si CP NMR for the roughly graphic illustration (non-quantitative).

A large Q^3 signal at -102 ppm was observed on the ^{1}H-^{29}Si CP NMR spectrum of the parent sample (Figure 2d) due to the presence of a significant number of silanol defects.[21, 23b] Conversely, the Q^3 signals became much smaller on the treated samples that are consistent with the FTIR spectra results, indicating that silanol defects of the parent sample were healed during LPST, consistent with the FTIR spectra results. on the MOR-400C sample, the Q^3 signal is a little more intense than other treated samples, possibly due to that some of the silanol defects in 8-MR are difficult to be reached at a lower temperature (Figure 2e). It is also observed that the Si(OAl)(OSi)$_3$ peaks in ^{29}Si NMR spectra were almost unchanged for the MOR-400C comparison with the parent sample, while the Q^4 peak corresponding to the Si in T_2+T_4 sites significantly increased along with the decrease of Q^3 species, suggesting that the reaction between $SiCl_4$ and silanol defects should be easier than the replacement of framework Al by $SiCl_4$ in the 12-MR channels.

Encouraged by ^{29}Si NMR, we could testify that the isomorphous substitution of Si for Al selectively occurs in 12-MR channels of MOR zeolites, which is the crucial step (extraction of undesired framework Al) of our proposed strategy. However, it is difficult to give more detailed T-site occupancy due to that the Q^4 resonance signals corresponding to Si in T_2 and T_4 sites are roughly overlapped. So that we try to use ^{27}Al MAS NMR and 2D ^{27}Al multiple-quantum magic-angle spinning (MQMAS) NMR techniques to solve the problem,[25] although the technique hardly distinguishes the framework Al occupancy at different T-sites of MOR zeolites due to its singlet signal in ^{27}Al NMR spectra.[4b, 26]

Figure 3 shows the ^{27}Al MAS NMR spectra acquired at 18.8 T of the MOR samples before and after the LPST. The NMR region related to the four-coordinated framework Al of MOR zeolites spans 45-65 ppm (Figure 3a).[27] For all the samples, there was no discernible indication could be observed corresponding to octahedral coordination Al (0-10 ppm region), five-coordinated Al (30-40 ppm region), and distorted tetrahedral Al (40-50 ppm region), respectively,[23a, 28] indicating that almost all Al atoms are located in the framework as tetrahedrally coordinated species. Figure 3b shows the region for the tetrahedral Al signals with NMR chemical shifts obtained for four nonequivalent T-sites as reference. All samples show a similar shape of Al NMR peaks, but a visible upfield shift of the tetrahedral Al signals was observed for the treated samples, indicating that the Al distribution in different T-sites is changed during LPST. It is noteworthy that a new peak at around 57.4 ppm raised on the spectrum of the MOR-600C sample, which may open up the possibility to distinguish different Al T-sites of MOR zeolite by ^{27}Al MAS NMR.

The MOR-600 sample was analyzed by 2D ^{27}Al MQMAS NMR for restraining and correctly dealing with the quadrupolar effect of ^{27}Al. Figure 3d shows the MQ NMR spectrum collected at 18.8 T, revealing several chemical shifts corresponding to different Al environments. Based on the isotropic chemical shifts (δ_{iso}) and the second-order quadrupolar coupling constant (C_Q) (Figure S10 and Table S4) obtained from the isotropic projection (F1) and the application of known methods for shearing,[29] the resonance signal at 45-65 ppm in the ^{27}Al NMR spectra of all MOR samples can be deconvoluted into four components at 56.2, 57.3, 58.4, and 60.3 ppm, owing to Al occupancy at four nonequivalent T-sites of MOR zeolites, called Al_a, Al_b, Al_c, and Al_d, respectively (Figure 3c and 3d). A quantitative evaluation of Al in each T-sites was obtained by combining XRF and ^{27}Al NMR (Figure 3g and Table S5) results, and the ratios in four framework Al species of parent MOR zeolite were that: Al_a > Al_b > Al_c > Al_d. The experiments and theoretical calculations have suggested that the framework Al are preferentially located in T_3 and T_4 sites of MOR

10.1002/anie.202116990

zeolite, and the order of Al occupancy at the T-sites obtained by all calculated methods is the same: $T_3 > T_4 > T_1 > T_2$.[5b, 26, 30] Thus, Al_c and Al_d can be unambiguously assigned to framework Al occupancy at T_1 and T_2 sites, respectively. Moreover, the Al_a and Al_b signals can be related to framework Al in T_3 and T_4 sites, but the intensities of the two signals are too similar to draw immediate conclusions about the exact contributions of Al_a and Al_b species.

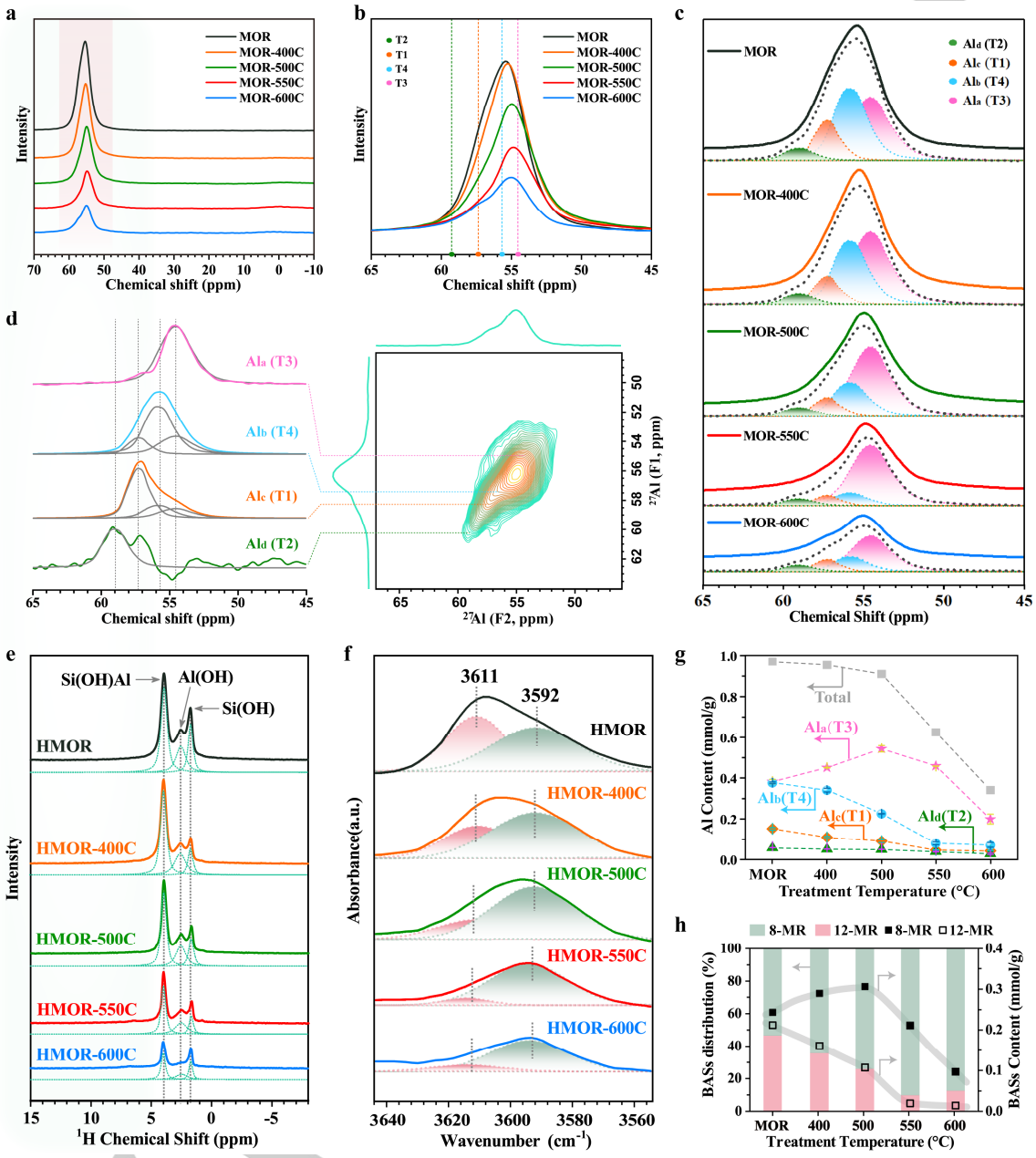

Figure 3. a) ^{27}Al MAS NMR spectra of all samples at 18.8 T magnetic field strengths. The region for the tetrahedral Al signal is enlarged in (b), and the chemical shift values for the four T-sites of MOR zeolite obtained from below are shown for reference. c) The deconvolution of the ^{27}Al MAS NMR spectra of as-made MOR zeolites. d) ^{27}Al MQMAS NMR spectrum of the MOR-600C sample at 18.8 T, and the slices extracted from F1 dimension. The acidity of catalysts was detected by ^{1}H MAS NMR (e) and FTIR (f) spectra. g) The evolution of zeolite framework Al atoms with increasing treatment temperature and the provided data of framework Al contents are determined from the combination of XRF and ^{27}Al MAS NMR (error bar from reproduced experiments in Table S8). h) The distributions and numbers of BASs in different channels of MOR samples with increasing treatment temperature and the provided data are determined from the combination of ^{1}H MAS NMR and FTIR.

The location of framework Al of zeolites determines the distribution of BASs.[25a, 31] The BASs in 8-MR channels of MOR zeolite are mainly originated by framework Al in T_3 sites, and the Brønsted H^+ corresponding to framework Al in T_4 sites are in 12-MR channels.[5b] Therefore, the information of Al siting can be further identified by the distribution of BASs. Figure 3e shows ^{1}H MAS NMR spectra of proton form of all MOR (HMOR) samples. Three primary resonance peaks at 3.8, 2.6, and 1.8 ppm were

observed, which can be assigned to the signals arising from the bridging hydroxyl (Si-OH-Al) groups, extra-framework Al hydroxyl (Al-OH) groups, and silanol (Si-OH) groups, respectively.[32] FTIR spectra of the samples show highly asymmetric bridging Si-OH-Al bands (3608 cm^{-1}) in the OH stretching region, which can be deconvoluted to two signals at 3611 and 3592 cm^{-1}, corresponding to stretching vibration of the Si-OH-Al groups in the 12-MR and 8-MR channels, respectively (Figure 3f).[7a, 10b] Thus, the quantitative estimation of BASs within the different channels of all HMOR catalysts was obtained by combining ^{1}H MAS NMR and FTIR (Table S6). Compared with the parent materials, the number of BASs in 8-MR channels exhibited a first increase and then decrease trend with increasing treatment temperature and had the maximum increment in the HMOR-500C sample (Figure 3h), owing to the change of framework Al in T_3 sites, which is consistent with the variation trend of Al_a signal. Hence the signal Al_a can be determinately assigned to framework Al in T_3 sites. The signal Al_b can be associated with Al in T_4 sites, whose gradually decreasing trend is also in line with the BASs in 12-MR channels. As shown above, based on the treated samples, the framework Al in different T-sites of MOR zeolites can be distinguished by high-filed ^{27}Al NMR combined with acid sites analysis, which is essential for understanding the location of framework Al in MOR zeolites.

After LPST, the decreases of the framework Al in T_1, T_2, and T_4 sites corresponding to 12-MR channels of MOR zeolite were observed (Figure 3g), owing to the replacement of undesired framework Al by Si in 12-MR channels, consistent with the ^{29}Si MAS NMR result. By contrast, the amounts of Al occupancy at T_3 sites increase significantly (maximum increase by about 43% in the MOR-500 sample), and the increase shows a good correlation with the healing of silanol defects in the 8-MR channels (Figure 2e), indicating that the Al extracted from 12-MR channels as $AlCl_3$ can migrate into the 8-MR channels and directly reinsert into T_3 sites as new framework Al through the reaction between the $AlCl_3$ and silanol defects. The formation of $AlCl_3$, which is small enough to access the 8-MR channels of MOR, is of primary importance for moving the framework Al into the desired T_3 sites. To further elucidate the formation of $AlCl_3$ during the LPST, we treated the parent MOR sample via external vaper $AlCl_3$. The amounts of framework Al in T_3 sites increase significantly with the consumption of the silanol defects (Figure S11), revealing that the extracted Al atoms from 12-MR in the form of $AlCl_3$ could be introduced into T_3 sites of MOR zeolites. The presence of silanol defects in T_3 sites provides positions for Al inserting into the zeolite framework. It is also evidenced that the LPST cannot cause the increase of framework Al in T_3 sites after healing the silanol defects in advance via the external vapor $AlCl_3$ treatment (Figure S13). For the MOR-400C sample, the amounts of framework Al are similar to the parent one, whereas the framework Al siting is distinctly changed, suggesting that the Al species extracted from 12-MR preferentially insert into T_3 sites rather than release from zeolites. In the MOR-550C sample, most of the framework Al are preferentially located into T_3 sites to 73%, which principally originates reactively favorable active sites (about 90%) in 8-MR channels (Figure 3h). At higher treatment temperature, since the number of extracted framework Al exceeded the capacities of silanol defects, part of Al as a form of $AlCl_3$ would be released from the channels of zeolite. It was evidenced by the unique diffraction peaks of $AlCl_3$ species in the XRD pattern of the collected products (Figure S12). Note that a distinct decrease in Al occupancy at T_3 sites was also observed in the MOR-600C sample because some $SiCl_4$ molecules access the 8-MR channels and replace framework Al at such elevated treatment temperature, consistent with the increase of Si occupancy at T_3 sites reflected by ^{29}Si NMR.

The resonance signal at 2.6 ppm was observed in ^{1}H MAS NMR spectra (Figure 3e), which indicates the presence of the extra-framework Al species in all HMOR samples, also evidenced by the sharp resonance signals at 0 ppm in ^{27}Al MAS NMR spectra (Figure S8c) and the stretching vibrations at 3660 cm^{-1} in FTIR spectra (Figure S7b) of the HMOR samples.[4b, 4d] In conjunction with Figure 3a, it could be demonstrated that despite almost all Al are located in the framework as tetrahedrally coordinated species for all samples in sodium form during the LPST, a fraction of Al was also removed from the zeolite framework in the following ammonium exchange process, in line with the conclusions of Ravi et al.[4b]

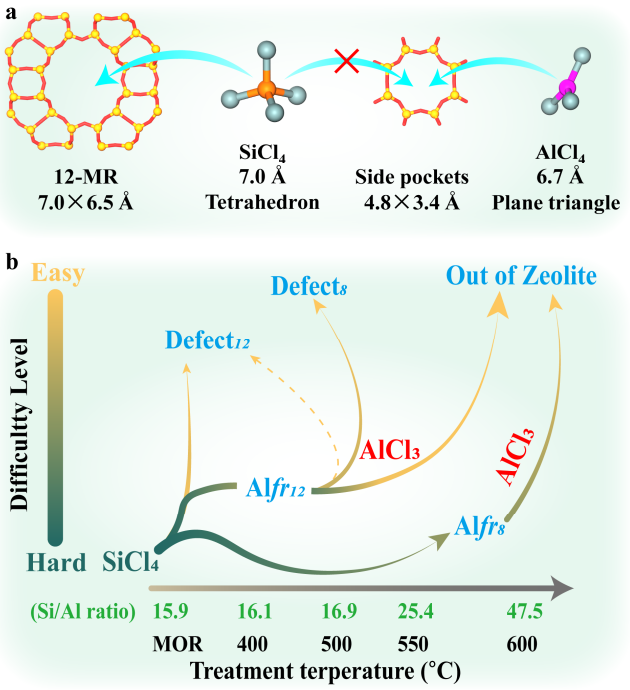

Figure 4. a) Compared size for $SiCl_4$ and $AlCl_3$ passing through the 12- and 8-MR channels of MOR zeolites, respectively. b) A complete picture of LPST reaction networks with diversely cooperative or competitive processes along with the evolution of framework composition.

All the results suggest that tandem reactions, involving selective extraction, migration, and reinsertion of Al in zeolite framework, occurred in different positions of the MOR zeolites in our proposed LPST strategy. We could draw an entire picture of the change of framework compositions for the samples before and after LPST with increasing treatment temperature, for further inferring the treated reaction networks with diversely cooperative or competitive processes along with the evolution of framework compositions (Scheme 1 and Figure 4b). Due to the molecular size, $SiCl_4$ (7.0 Å, tetrahedron configuration) can selectively access 12-MR (7.0 × 6.5 Å) rather than 8-MR (5.7 × 2.6 Å) channels (Figure 4a). As $SiCl_4$ molecules diffuse slowly and steadily into the 12-MR, they preferentially react with silanol

defects in 12-MR (Defect$_{12}$) to incorporate Si into the framework position and heal the zeolite defects. Then, $SiCl_4$ molecules further react with the framework Al in 12-MR (Al$_{fr12}$) with the release of $AlCl_3$. That is to say, the undesired framework Al is extracted as a form of $AlCl_3$ via replacing by Si. The $AlCl_3$ (6.7 Å) molecule, which is more easily distorted owing to its plane triangle configuration, can migrate into 8-MR channels through the side pockets (4.8 × 3.4 Å) and react with silanol defects of 8-MR channels (Defect$_8$) to insert Al into T_3 sites as tetrahedrally coordinated species. With the increasing treatment temperature, more $AlCl_3$ extracted from the zeolite framework exceed the amounts of defects in 8-MR that provide the position for Al reinserting into the framework. The exceeded $AlCl_3$ are released out of zeolite, encouraged by the significant increase of Si/Al ratio. At elevated treatment temperature (600 °C), some $SiCl_4$ could also access 8-MR channels and replace framework Al (Al$_{fr8}$), evidenced by the decrease of Al siting in T_3 sites. Ultimately, this treatment leads to the framework Al selective occupancy at T_3 sites, a specific position in the given channel of MOR zeolite for achieving a singularly unique catalytic selectivity.

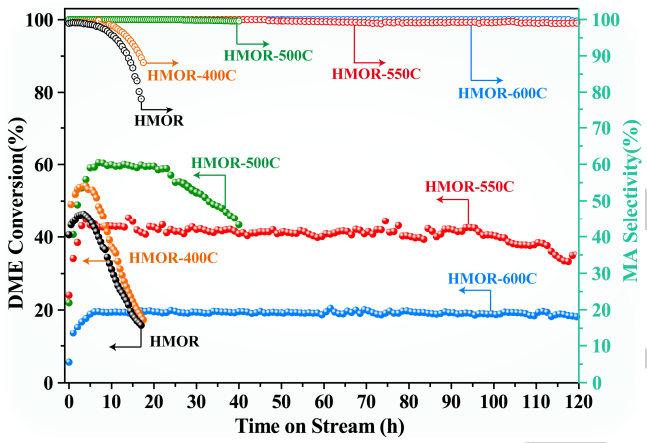

Figure 5. DME conversion and MA selectivity over the parent and treated HMOR catalysts. Reaction conditions: 200 °C, 2Mpa, DME/CO/N_2 = 2/48/50, GHSV=2400 ml/g/h.

As shown in Figure 5, the carbonylation of DME to MA reaction, which is sensitive to the distribution of BASs within different positions of MOR zeolites,[7a, 8, 33] is significantly different on the parent and treated MOR catalysts. Remarkably, the DME conversion firstly increased and then decreased with the increasing treatment temperature. Figure S15a shows a linear correlation between the yield of MA and BASs capacity within 8-MR channels for all samples, consistent with the reported by other researchers.[7a, 33a]

Another striking observation is the significantly longer catalytic lifetime of the treated samples, especially on the HMOR-550C and HMOR-600C samples, being stable for at least 25 times longer than the parent HMOR catalyst. These samples have much lower BASs capacity in 12-MR channels, which are responsible for the coke formation and frequent deactivation.[18a, 34] With this information in hand, it is essential to increase the acidity in 8-MR and remove of acidity of 12-MR channels for a high-activity and long-lived MOR catalyst in DME carbonylation reaction. The controllable relocation of framework Al determines the desirable acidity distribution in different positions of MOR zeolites for DME carbonylation reaction via our proposed strategy. In return, all catalytic results also point to conclusions similar to those from the systematic characterizations on the distribution of framework Al and acid sites.

Conclusion

In summary, Low-pressure $SiCl_4$ treatment (LPST) strategy was developed to selectively direct framework Al into targeted T_3 sites of MOR zeolites in this work. The information of framework Al siting in treated MOR zeolites was identified using high-field ^{27}Al NMR combined with the analysis of active sites. The analyses show that this approach realizes directional move of Al from 12-MR to 8-MR channels through selective extraction of undesired framework Al in 12-MR, oriented migration of extracted Al species ($AlCl_3$) from 12-MR to 8-MR, and reinsertion of Al into targeted T_3 positions in 8-MR channels.

The developed strategy selectively locates most of the framework Al into T_3 sites of the synthetic MOR zeolites, which provides an excellent catalytic environment with the unique active sites in 8-MR channels for DME carbonylation reaction, and leads to the significantly longer catalytic lifetime and higher selectivity of MA. This approach for tailoring catalysts to optimize the location of framework Al has been effectively applied in MOR zeolites and could be extended to other zeolites to favour the enhancement of catalytic performance based on the achievement of the specifically required location of active species in the catalysts.

Acknowledgements

This work was supported by the National Natural Science Foundation of China (Nos. 21991090, 21991093, 21991091, and 22022202), The International Partnership Program of Chinese Academy of Sciences (121421KYSB20180007), the Key Research Program of Frontier Sciences, CAS, Grant No. QYZDY-SSW-JSC024.

Conflict of interest

The authors declare no conflict of interest.

Keywords: active sites • aluminum • catalysts design • DME carbonylation • zeolites

[1] C. S. Cundy, P. A. Cox, *Chem. Rev.* **2003**, *103*, 663-702.
[2] K. Muraoka, W. Chaikittisilp, T. Okubo, *J. Am. Chem. Soc.* **2016**, *138*, 6184-6193.
[3] J. Dedecek, E. Tabor, S. Sklenak, *Chemsuschem* **2019**, *12*, 556-576.
[4] a) X. M. Tang, Z. Q. Liu, L. Huang, W. Chen, C. B. Li, G. R. Wang, G. C. Li, X. F. Yi, A. M. Zheng, *ACS Catal.* **2019**, *9*, 10618-10625; b) M. Ravi, V. L. Sushkevich, J. A. van Bokhoven, *Chem. Sci.* **2021**, *12*, 4094-4103; c) B. C. Knott, C. T. Nimlos, D. J. Robichaud, M. R. Nimlos, S. Kim, R. Gounder, *ACS Catal.* **2018**, *8*, 770-784; d) T. T. Le, A. Chawla, J. D. Rimer, *J. Catal.* **2020**, *391*, 56-68; e) M. Ravi, V. L. Sushkevich, J. A. van Bokhoven, *Nat. Mater.* **2020**, *19*, 1047-1056.
[5] a) Y. Li, S. Y. Huang, Z. Z. Cheng, K. Cai, L. D. Li, E. Milan, J. Lv, Y. Wang, Q. Sun, X. B. Ma, *Appl. Catal. B* **2019**, *256*, 117777; b) H. Huo, L. Peng, Z. Gan, C. P. Grey, *J. Am. Chem. Soc.* **2012**, *134*, 9708-9720.

[6] a) M. Boronat, C. Martinez, A. Corma, *Phys. Chem. Chem.Phys.* **2011**, *13*, 2603-2612; b) D. B. Lukyanov, T. Vazhnova, N. Cherkasov, J. L. Casci, J. J. Birtill, *J. Phys. Chem. C* **2014**, *118*, 23918-23929.

[7] a) A. Bhan, A. D. Allian, G. J. Sunley, D. J. Law, E. Iglesia, *J. Am. Chem. Soc.* **2007**, *129*, 4919-4924; b) P. Cheung, A. Bhan, G. J. Sunley, E. Iglesia, *Angew. Chem. Int. Ed.* **2006**, *45*, 1617-1620; c) R. Gounder, E. Iglesia, *J. Am. Chem. Soc.* **2009**, *131*, 1958-1971; d) F. Jiao, X. L. Pan, K. Gong, Y. X. Chen, G. Li, X. H. Bao, *Angew. Chem. Int. Ed.* **2018**, *57*, 4692-4696.

[8] M. Boronat, C. Martinez-Sanchez, D. Law, A. Corma, *J. Am. Chem. Soc.* **2008**, *130*, 16316-16323.

[9] a) R. Gounder, E. Iglesia, *Angew. Chem. Int. Ed.* **2010**, *49*, 808-811; b) A. Bhan, E. Iglesia, *Acc. Chem. Res.* **2008**, *41*, 559-567; c) E. S. Zhan, Z. P. Xiong, W. J. Shen, *J. Energy Chem.* **2019**, *36*, 51-63.

[10] a) Y. Zhang, X. San, N. Tsubaki, Y. Tan, J. Chen, *Ind. Eng. Chem. Res.* **2010**, *49*, 5485-5488; b) K. P. Cao, D. Fan, L. Y. Li, B. H. Fan, L. Y. Wang, D. L. Zhu, Q. Y. Wang, P. Tian, Z. M. Liu, *ACS Catal.* **2020**, *10*, 3372-3380.

[11] a) J. Dedecek, V. Balgova, V. Pashkova, P. Klein, B. Wichterlova, *Chem. Mater.* **2012**, *24*, 3231-3239; b) V. Pashkova, P. Klein, J. Dedecek, V. Tokarova, B. Wichterlova, *Microporous Mesoporous Mater.* **2015**, *202*, 138-146; c) T. Yokoi, H. Mochizuki, S. Namba, J. N. Kondo, T. Tatsumi, *J. Phys. Chem. C* **2015**, *119*, 15303-15315; d) T. Y. Liang, J. L. Chen, Z. F. Qin, J. F. Li, P. F. Wang, S. Wang, G. F. Wang, M. Dong, W. B. Fan, J. G. Wang, *ACS Catal.* **2016**, *6*, 7311-7325; e) V. Pashkova, S. Sklenak, P. Klein, M. Urbanova, J. Dedecek, *Chem. Eur. J.* **2016**, *22*, 3937-3941.

[12] a) J. R. Di Iorio, C. T. Nimlos, R. Gounder, *ACS Catal.* **2017**, *7*, 6663-6674; b) J. R. Di Iorio, R. Gounder, *Chem. Mater.* **2016**, *28*, 2236-2247; c) J. R. Di Iorio, S. C. Li, C. B. Jones, C. T. Nimlos, Y. J. Wang, E. Kunkes, V. Vattipalli, S. Prasad, A. Moini, W. F. Schneider, R. Gounder, *J. Am. Chem. Soc.* **2020**, *142*, 4807-4819.

[13] a) A. B. Pinar, C. Marquez-Alvarez, M. Grande-Casas, J. Perez-Pariente, *J. Catal.* **2009**, *263*, 258-265; b) Y. Román-Leshkov, M. Moliner, M. E. Davis, *J. Phys. Chem. C* **2011**, *115*, 1096-1102.

[14] M. Liu, T. Yokoi, M. Yoshioka, H. Imai, J. N. Kondo, T. Tatsumi, *Phys. Chem. Chem. Phys.* **2014**, *16*, 4155-4164.

[15] a) Y. Li, M. Yu, K. Cai, M. Y. Wang, J. Lv, R. F. Howe, S. Y. Huang, X. B. Ma, *Phys. Chem. Chem. Phys.* **2020**, *22*, 11374-11381; b) L. Y. Li, Q. Y. Wang, H. C. Liu, T. T. Sun, D. Fan, M. Yang, P. Tian, Z. M. Liu, *ACS Appl. Mater. Interfaces* **2018**, *10*, 32239-32246.

[16] F. F. Gao, M. Jaber, K. Bozhilov, A. Vicente, C. Fernandez, V. Valtchev, *J. Am. Chem. Soc.* **2009**, *131*, 16580-16586.

[17] a) C. D. Chang, C. T. W. Chu, J. N. Miale, R. F. Bridger, R. B. Calvert, *J. Am. Chem. Soc.* **1984**, *106*, 8143-8146; b) S. Namba, K. Yamagishi, T. Yashima, *Chem. Lett.* **1987**, 1109-1112; c) K. J. Yamagishi, S. Namba, T. Yashima, *J. Catal.* **1990**, *121*, 47-55; d) P. Wu, T. Komatsu, T. Yashima, *J. Phys. Chem.* **1995**, *99*, 10923-10931; e) J. J. Li, M. Liu, X. W. Guo, C. Y. Dai, S. T. Xu, Y. X. Wei, Z. M. Liu, C. S. Song, *Ind. Eng. Chem. Res.* **2018**, *57*, 8190-8199.

[18] a) A. A. C. Reule, J. A. Sawada, N. Semagina, *J. Catal.* **2017**, *349*, 98-109; b) M. C. Silaghi, C. Chizallet, J. Sauer, P. Raybaud, *J. Catal.* **2016**, *339*, 242-255.

[19] a) H. K. Beyer, I. Belenykaja, in *Stud. Surf. Sci. Catal., Vol. 5* (Eds.: B. Imelik, C. Naccache, Y. B. Taarit, J. C. Vedrine, G. Coudurier, H. Praliaud), Elsevier, **1980**, pp. 203-210; b) J. A. Martens, H. Geerts, P. J. Grobet, P. A. Jacobs, *J. Chem. Soc., Chem. Commun.* **1990**, 1418-1419; c) J. Klinowski, J. M. Thomas, M. W. Anderson, C. A. Fyfe, G. C. Gobbi, *Zeolites* **1983**, *3*, 5-7; d) P. Bartl, W. F. Holderich, *Microporous Mesoporous Mater.* **2000**, *38*, 279-286.

[20] a) H. K. Beyer, *Post-Synthesis Modification I* **2002**, *3*, 203-255; b) M. Muller, G. Harvey, R. Prins, *Microporous Mesoporous Mater.* **2000**, *34*, 135-147.

[21] S. Prodinger, M. A. Derewinski, A. Vjunov, S. D. Burton, I. Arslan, J. A. Lercher, *J. Am. Chem. Soc.* **2016**, *138*, 4408-4415.

[22] P. Losch, H. R. Joshi, O. Vozniuk, A. Grünert, C. Ochoa-Hernández, H. Jabraoui, M. Badawi, W. Schmidt, *J. Am. Chem. Soc.* **2018**, *140*, 17790-17799.

[23] a) A. Vjunov, M. A. Derewinski, J. L. Fulton, D. M. Camaioni, J. A. Lercher, *J. Am. Chem. Soc.* **2015**, *137*, 10374-10382; b) K. Iyoki, K. Kikumasa, T. Onishi, Y. Yonezawa, A. Chokkalingam, Y. Yanaba, T. Matsumoto, R. Osuga, S. P. Elangovan, J. N. Kondo, A. Endo, T. Okubo, T. Wakihara, *J. Am. Chem. Soc.* **2020**, *142*, 3931-3938.

[24] W. Kolodziejski, P. J. Barrie, H. He, J. Klinowski, *J. Chem. Soc., Chem. Commun.* **1991**, 961-962.

[25] a) Z. J. Berkson, M. F. Hsieh, S. Smeets, D. Gajan, A. Lund, A. Lesage, D. Xie, S. I. Zones, L. B. McCusker, C. Baerlocher, B. F. Chmelka, *Angew. Chem. Int. Ed.* **2019**, *58*, 6255-6259; b) A. Vjunov, J. L. Fulton, T. Huthwelker, S. Pin, D. Mei, G. K. Schenter, N. Govind, D. M. Camaioni, J. Z. Hu, J. A. Lercher, *J. Am. Chem. Soc.* **2014**, *136*, 8296-8306; c) K. Chen, S. Horstmeier, V. T. Nguyen, B. Wang, S. P. Crossley, T. Pham, Z. Gan, I. Hung, J. L. White, *J. Am. Chem. Soc.* **2020**, *142*, 7514-7523; d) S. Sklenak, J. Dedecek, C. B. Li, B. Wichterlova, V. Gabova, M. Sierka, J. Sauer, *Angew. Chem. Int. Ed.* **2007**, *46*, 7286-7289; e) S. Sklenak, J. Dedecek, C. Li, B. Wichterlova, V. Gabova, M. Sierka, J. Sauer, *Phys. Chem. Chem. Phys.* **2009**, *11*, 1237-1247.

[26] M. Jeffroy, C. Nieto-Draghi, A. Boutin, *Chem. Mater.* **2017**, *29*, 513-523.

[27] J. Barras, J. Klinowski, D. W. McComb, *J. Chem. Soc., Faraday Trans.* **1994**, *90*, 3719-3723.

[28] a) J. A. van Bokhoven, D. C. Koningsberger, P. Kunkeler, H. van Bekkum, A. P. M. Kentgens, *J. Am. Chem. Soc.* **2000**, *122*, 12842-12847; b) J. Pérez-Pariente, J. Sanz, V. Fornés, A. Corma, *J. Catal.* **1990**, *124*, 217-223.

[29] O. H. Han, C. S. Kim, S. B. Hong, *Angew. Chem. Int. Ed.* **2002**, *41*, 469-472.

[30] a) K. Shiokawa, M. Ito, K. Itabashi, *Zeolites* **1989**, *9*, 170-176; b) J. L. Schlenker, J. J. Pluth, J. V. Smith, *Mater. Res. Bull.* **1979**, *14*, 751-758; c) A. Alberti, *Zeolites* **1997**, *19*, 411-415; d) J. B. Jones, *Acta Crystallographica Section B-Structural Crystallography and Crystal Chemistry* **1968**, *B 24*, 355-&; e) A. Alberti, G. Gottardi, T. Lai, (Eds.: D. Barthomeuf, E. G. Derouane, W. Hölderich), Springer US, Boston, MA, **1990**, pp. 145-155.

[31] C. G. Li, A. Vidal-Moya, P. J. Miguel, J. Dedecek, M. Boronat, A. Corma, *ACS Catal.* **2018**, *8*, 7688-7697.

[32] a) X. Yi, Y. Xiao, G. Li, Z. Liu, W. Chen, S.-B. Liu, A. Zheng, *Chem. Mater.* **2020**, *32*, 1332-1342; b) T. He, X. Liu, S. Xu, X. Han, X. Pan, G. Hou, X. Bao, *J. Phys. Chem. C* **2016**, *120*, 22526-22531.

[33] a) J. Liu, H. Xue, X. Huang, P.-H. Wu, S.-J. Huang, S.-B. Liu, W. Shen, *Chin. J. Catal.* **2010**, *31*, 729-738; b) H. F. Xue, X. M. Huang, E. Ditzel, E. S. Zhan, M. Ma, W. J. Shen, *Chin. J. Catal.* **2013**, *34*, 1496-1503; c) Z. Q. Liu, X. F. Yi, G. R. Wang, X. M. Tang, G. C. Li, L. Huang, A. M. Zheng, *J. Catal.* **2019**, *369*, 335-344.

[34] H. F. Xue, X. M. Huang, E. Ditzel, E. S. Zhan, M. Ma, W. J. Shen, *Ind. Eng. Chem. Res.* **2013**, *52*, 11510-11515.

10.1002/anie.202116990

WILEY-VCH

RESEARCH ARTICLE

Table of Contents

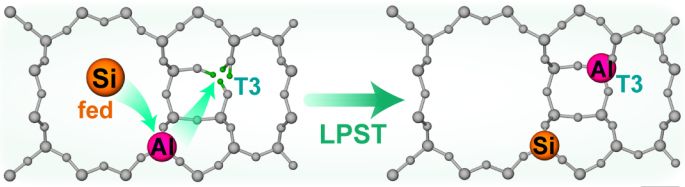

After a low-pressure $SiCl_4$ treatment (LPST), the undesired framework aluminum atoms in the 12-MR channels of a MOR zeolite migrate to the desired T_3 sites to increase the number of favorable active sites